Analysis of Design and Operation of Multi-Point Ground Flares

Joseph Smith[¥], Ahti Suo-Anttila[§], Zach Smith[ɬ], Vikram Sreedharan[ɬ]

[¥]*Chemical and Biochemical Engineering, Missouri Univ of Sci and Tech, Rolla, MO 65409 USA*
[§]*Computational Engineering Analysis LLC, 4729 Paso Del Puma Ne, Albuquerque, NM 87111 USA*
[ɬ]*Elevated Analytics Consulting, 343 East 4th Street, Suite 104, Rexburg, ID 83440 USA*

Abstract

Multi-point ground flares (MPGF) are used to process large quantities of hydrocarbon gases generated in chemical processing or petrochemical refining. These flares use hundreds of flare burners arranged and fired in a staged fashion. A wind fence surrounds the MPGF to shield the flames from plant operators and neighboring communities reduce the impact of ambient wind on the flames to promote highly efficient combustion-(see Figure 1). Safety concerns related to radiation flux, ignition cross lighting, and excessive emissions have been examined using Computational Fluid Dynamics (CFD) [1]. This paper will discuss recent work aimed at understanding how burner and row spacing impact radiation flux and respective ground and fence temperature plus flame shape and height. Based on previous work, design guidelines and operating limits are being developed addressing:

- Flame height, shape and smokeless performance based on tip spacing and row spacing,
- Wind fence porosity and its impact on flame height and soot production,
- Tip port area and tip spacing effect on predicted radiation flux surrounding surfaces,
- Tip size effect on flare DRE and ignition, and
- Radiation flux outside of the wind fence.

Previous work on MPGF design and operation supporting these conclusions is discussed.

Figure 1 – General Multi-Point Ground Flare (MPGF) with tips and wind fence design

INTRODUCTION

Low profile Multi-Point Ground flares (MPGF) represent a special class of flares capable of safely processing significant quantities of flare gas in an environmentally responsible fashion. These flare systems often involve hundreds of burners arranged in rows for staged operation to handle large firing rates. They are generally located away from the main plant or refinery to reduce potential damage to surrounding equipment (see Figure 2). Using detailed computational fluid dynamics (CFD) simulation, a MPGF design can be analyzed to evaluate various challenges associated with specific operating conditions and to explore various design options to ensure highly efficient operation.

Figure 2 –MPGF are generally located away from main plant to prevent damage to surround equipment

Often, a MPGF is designed to fire large amounts of flammable hydrocarbon gas. These flares must also operate in low flow "purge" conditions which allows them to be in a 'hot-standby' mode in case they must quickly respond to emergency firing conditions. At high firing rates, the associated high heat release from the flare creates high thermal radiation flux to surrounding surfaces (i.e., wind fence, runners, gravel, piping, and cable trays). MPGF's can also produce high soot levels and large clouds of unburnt hydrocarbons. The potential safety and environmental hazards associated with MPGFs have been evaluated using C3d.

Over the past several years, engineers at Elevated Analytic Consulting have analyzed over many MPGF systems using the proprietary transient LES based CFD tool called *C3d*. This tool has been used to analyze other flare types as well including enclosed flares, elevated steam and air-assisted flares, utility flares, and elevated pressure-assisted flares. In this paper we discuss the modeling methodology developed to simulate MPGF systems. In addition, we identify several design features shown to be important to safe, efficient operation of MPGFs that impact their overall performance.

Previous work has evaluated various MPGF system with specified wind fence design with burner and row spacing operating under varying ambient wind conditions (see Figure 3 and Figure 4). Code validation has also been performed and reported elsewhere that quantifies code accuracy [2], [3]. Work has also has focused on evaluating the combustion model used in these analyses to

properly approximate the complex turbulent reacting flow chemistry inherent in MPGF operation [4], [5], [6].

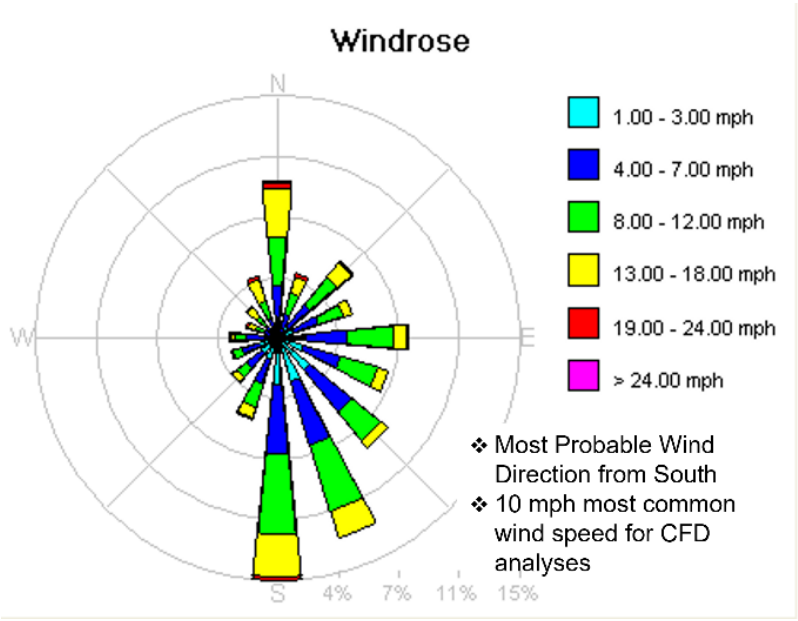

Figure 3 –Prevailing wind data

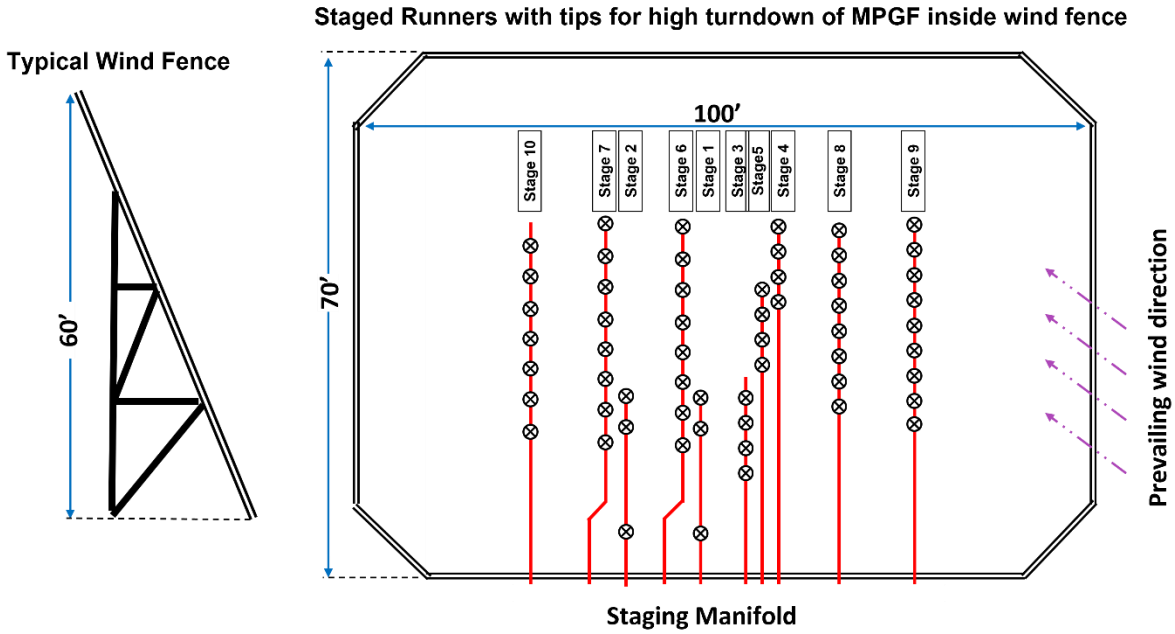

Figure 4 - Typical wind fence (LHS) with staged burner layout in rows (RHS)

General design questions related to an MPGF system include the burner tip spacing for efficient cross lighting along a runner, runner spacing to ensure adequate oxygen gets to the inner burners in a runner, burner tip flow area to maximize firing rate with the fewest burners, whether to use assist media to enhance flare gas mixing above each flare tip, and the specific wind fence design including the lower safety fence near ground level to ensure safe and efficient operation of the MPGF. The flare performance can be quantified using metrics such as % energy loss from the flame, soot and CO Iso-surfaces colored by temperature to visualize the flame, Flare destruction efficiency (DRE), and Fence and Ground Temperature among others. Based on the CFD analysis, general design and operating guidelines are suggested in this paper. This work may provide flare vendors and MPGF end-users with a basis for future MPGF designs and to ensure safe and efficient operation.

MODELING MULTI-POINT GROUND FLARES

The CFD tool used in this work simulates turbulent reaction chemistry coupled with radiative transport between buoyancy driven flames and nearby objects including wind fences, piping manifolds, pipe runners and adjacent burner tips. The code provides "reasonably" accurate risk estimates related to common failure scenarios including 1) flame impingement on adjacent burners, pipe runners, and the wind fence due to cross winds, 2) high soot production rates, 3) low DRE, and 4) high heat exposure of nearby operating personnel. Typical simulations of MPGFs using *C3d* generally require CPU times on the order of hours to a few days using a windows desktop workstation. Large Eddy Simulation (LES) has been shown to more accurately approximate turbulent mixing than standard Reynolds Averaged Navier Stokes (RANS) based CFD codes. [7] The current *C3d* code is based on an earlier CFD code called ISIS-3D [8]. ISIS-3D, originally developed at Sandia National Laboratory, has been commercialized into a user friendly CFD tool with a graphical user interface called *C3d*. This tool is specifically tailored to analyze MPGF performance. *C3d* has previously been applied to MPGFs as well as elevated multipoint flares, elevated air- and steam-assisted flares, and utility flares. [4] New combustion models have been developed, implemented, and tested for various flare gas compositions including methane, ethane, ethylene, propane, propylene, and xylene [3]. *C3d* has successfully predicted flame size and shape with soot formation from single and multiple test flare burners firing typical flare gas. The code also successfully predicted the radiation flux from the flame to surrounding radiometers used to measure radiation flux from the flame. These *C3d* simulation results of flame height and flame-to-ground radiation were validated by direct comparison to measured flame size, shape, and radiation measurements taken during single-burner and multi-burner tests conducted under no-wind and low-wind ambient conditions [5].

C3d simulations can be performed to analyze MPGF start-up, normal operation, and maximum firing rates subject to various wind speeds and direction. During these simulations, the impact that tip spacing has on ignition and cross lighting has been examined and reported earlier. [5] The impact that tip size in a cross wind has on % energy loss from the flame has also been investigated and reported earlier. [9] Several wind fence designs have also examined to

investigate its impact on air flow to the flare tip base. Predictions of wind fence temperature with heat loss from the backward face of the fence has also been investigated [10]. The expected flare destruction efficiency (DRE) has also been examined for various designs. These CFD analyses were done to investigate MPGF performance as a function of design and operating conditions. To ensure comparable results from each *C3d* simulation, the following methodology has been developed for each simulation.

Simulation Methodology

To ensure the flare is operating with a steady wind profile blowing over the flare, all transient simulations are run for approximately 10 to15 seconds of flare operating time (approximately 3-4 days CPU time) before initiating flare gas flow and combustion in the MPGF. Once the wind profile is established and flare gas is burning at a steady rate, the simulation is allowed to run for another 10-20 seconds of "burn-time" (2-3 days CPU time). This allows a full spectrum of representative flame fluctuations caused by interactions between the wind and the flare flame above the burners. The "burn time" represents flare operation in an essentially "quasi-steady-state" condition of 10 to 12 seconds flare operating time. Following this procedure, most MPGF CFD cases take approximately 5-7 CPU days to run and another 2-3 days to post-process results for subsequent analysis.

Since a transient solver is used in *C3d*, all field variables fluctuate in time due to turbulence and other non-linear effects caused by coupling between the partial differential equations describing conservation of mass, momentum, and energy in the MPGF. Using the procedure described above, "quasi-steady state" flare operation is confirmed when trends in the predicted variables stop increasing (decreasing) and exhibit random fluctuations associated with turbulent fluctuations in the flow field.

The convergence criteria chosen for all simulations is based on the equation of state always being satisfied to within 0.01% or less at any location in the computational domain. Typically, this convergence criterion is better than the maximum allowable error since the time step constraint is limited by the Courant condition, which allows the flow field to be solved to a higher degree of accuracy.

TECHNICAL APPROACH

Due to the size of the flare field, modeling the exact fence geometry for the full flare simulation is not practical since it would require an extremely fine computational mesh to properly resolve the slats and spaces in the fence and the associated CPU time to perform the transient LES CFD analyses would be prohibitive. Instead, we have developed and validated an approach to approximate detailed fence geometry using porous plates that approximate the actual fence geometry [4]. This method uses a detailed CFD analysis of a section of the fence to predict the pressure drop through a detailed fence model (see Figure 5). This pressure drop is used to set the

fence porosity in the porous plate approximation which is then used to include the fence impact on MPGF performance in cross winds.

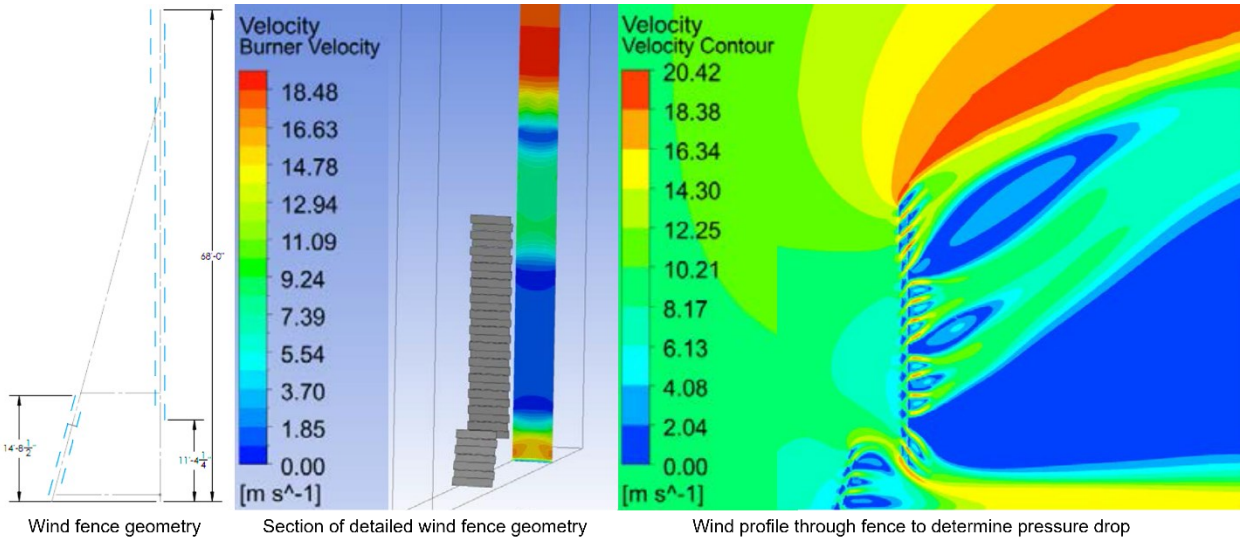

Figure 5 - Wind fence approximation method

More critical is the mesh refinement required to accurately simulate jet flow from a common flare burner tip (see Figure 6). Consider that most MPGF have more than 100 flare burner tips and that each burner tip has a minimum of 20 ports with the port diameter less than 1mm (0.039”). To simulate the jet flow profile from a single port would require 5 cells in the x and y direction across the port exit and extend at least 10 port diameters beyond the port exit with z-direction cells having a similar size as the x and y-direction cell have which means each port would require a minimum of at least 50 cells above the burner port. Thus, for each burner tip with 20 ports, 5 x 5 x 50 x 20 = 25,000 cells would be required for each per burner tip. For a flare field with 100 burners that represents at least 250,000 cells in the near burner region. Coupled with the cells to approximate the entire flare field with sufficient resolution upwind and downwind of the flare field and sufficient distance from the crosswind direction (-y-direction and +y-direction), a computational mesh would easily exceed 100,000,000 cells. This level of resolution would require excessive CPU time on a large High-Performance Computer (HPC) to complete a fully transient LES based CFD analysis for a MPGF. C3d is tailored to allow fully transient analysis of MPGF using mass sources located on each burner tip. Instead of resolving flow from individual jets using a refined mesh, *C3d* uses mass sources located on the burner face of each burner tip. This approach allows *C3d* to accurately capture individual jet flow dynamics along

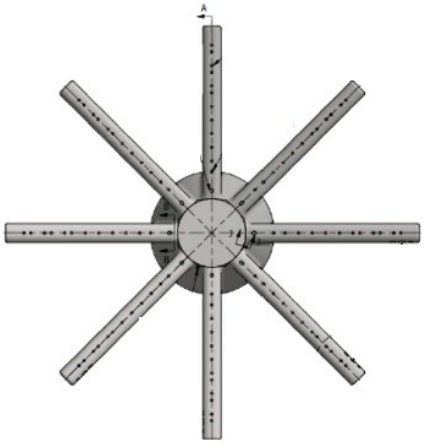

Figure 6 - MPGF nozzle used in validation tests

with coupling between adjacent jets from all burner tips in an MPGF simulation without having to resolve the flow dynamics using a refined mesh.

C3d uses a structured grid composed of hexahedral cells (see Figure 7) to approximate the MPGF geometry as well as nearby structures and/or topology (Figure 8). The size of the computational domain can be adjusted to avoid interaction from the domain boundaries that might impact predicted flame height or plume dispersion. In a steady-state RANS CFD analysis, the formal mesh independence study involves halving and doubling cell size in the computational domain. By comparison, *C3d* simulations are transient so mesh independence is checked using several different meshes with varying degrees of refinement near the burners and wind fence to check for mesh independence. Since the coupled transport processes are complicated by transient non-uniform wind and heat profiles, this approach to mesh independence confirmation has been effective. In *C3d* simulations of MPGF flames, the code is "tuned" using results from earlier validation cases. This required a full MPGF case use the same base mesh size as the validation case. This criterion establishes the relative cell size and resulting mesh density used in a MPGF case. The final grid for an overall MPGF flare analysis normally consisted of one to five million cells (with refinement near the burners) unless surrounding equipment is included which may also require clustered cells in areas of high flow gradients.

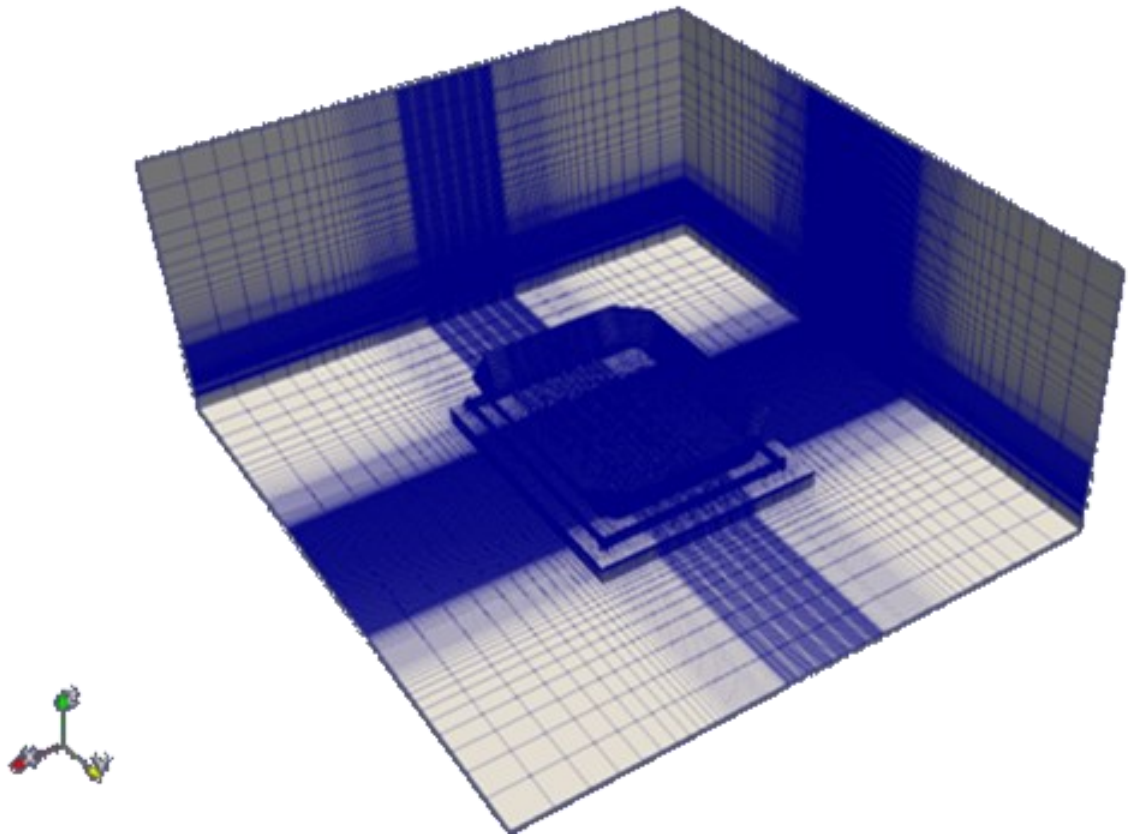

Figure 7 - Hexahedral mesh (3.34 million cells) with extended domain height to capture plume from MPGF

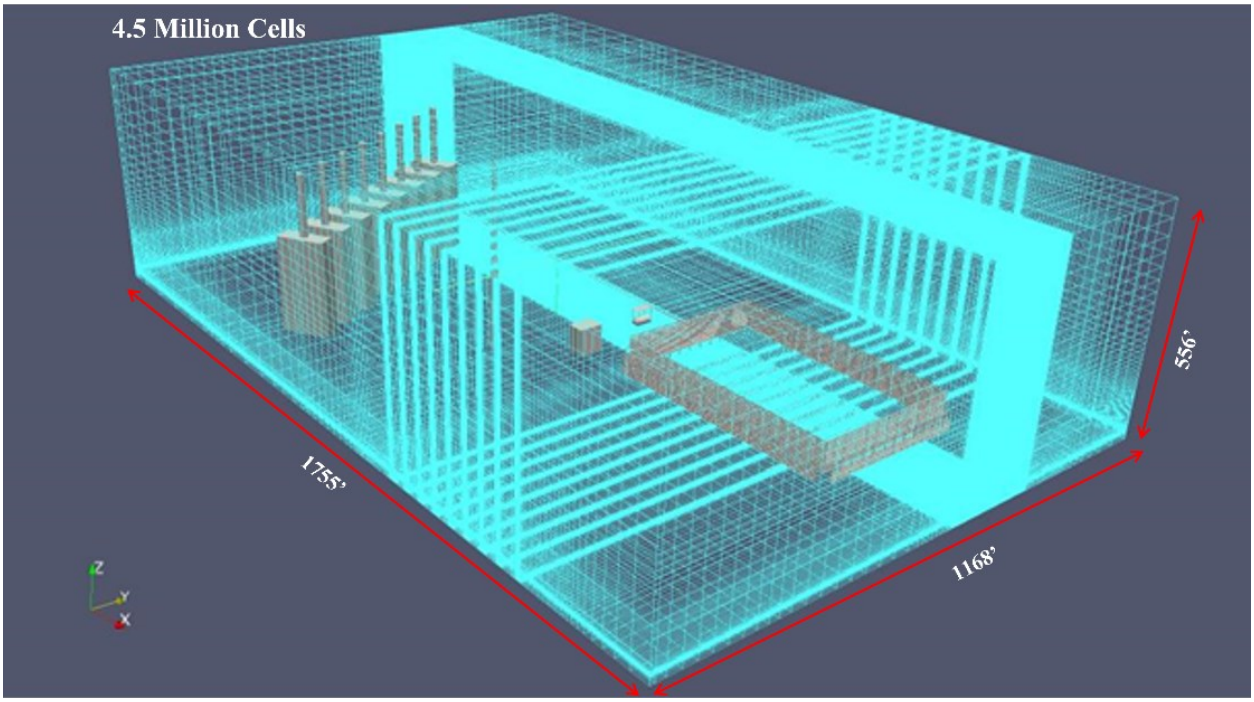

Figure 8 - Hexahedral mesh (4.5 million cells) with extended domain to capture impact of MPGF on surrounding equipment

Combustion Model

Global reaction kinetics are often used to model combustion as a single step in CFD combustion simulations. The stoichiometric coefficients and reaction constants are fit to measured rate data. Although it is possible to use a global reaction mechanism with the same coefficients as those published elsewhere, this could produce incorrect results since the published mechanism was developed with a specific set of kinetic data for a unique combustion experiment being modeled. It is well known that simulation results are sensitive to both the computational grid (cell size, aspect ratio, and number of cells) and the kinetic data used by the original authors to build the simplified combustion model. Hence, a new computational grid for a different application would likely require a different set of reaction coefficients.

To accurately model flare gas combustion, a consistent set of chemical reactions that describe the overall combustion chemistry is required. To minimize CPU requirements, a minimum number of chemical reactions should be identified and used to predict the total energy yield and species consumption and production. Based on heat transfer, flame size, and air demand the specific details of the chemical reactions used are not critical if the oxygen consumption is correctly balanced for a given fuel type and the amount of soot produced is calibrated to match experimental data and observation.

For systems burning complex mixtures of hydrocarbons, a "modified" combustion model covering a wide range of fuels and intermediate species has been developed and validated [3]. To

use this model, fuel combustion is separated into primary fuel breakdown reactions which form intermediate species followed by combustion of those intermediate species. Primary fuel breakdown reactions are shown in Eq. 1 –8 for a wide range of hydrocarbons:

$1.5C_2H_4 + 1.5O_2 \rightarrow CO + C_2H_2 + 2H_2O$ *Ethylene breakdown* (1)

$C_3H_8 + 1.5O_2 \rightarrow C_2H_2 + 2H_2O + CO + H_2$ *Propane breakdown* (2)

$C_2H_6 + 0.5O_2 \rightarrow 0.5C_2H_2 + CO + H_2$ *Ethane breakdown* (3)

$C_3H_4 + O_2 \rightarrow C_2H_2 + H_2O + CO$ *Propadiene breakdown* (4)

$C_5H_{12} + 4O_2 \rightarrow C_2H_2 + 5H_2O + 3CO$ *N-Pentane breakdown* (5)

$C_4H_6 + 4O_2 \rightarrow 2C_2H_2 + H_2O$ *1,2, Butadiene breakdown* (6)

$C_3H_6 + 1.5O_2 \rightarrow C_2H_2 + 2\ H_2O + CO$ *Propylene breakdown* (7)

$C_{12}H_{26} + 6.5O_2 \rightarrow 7H_2O + 2CH_4 + 2C_2H_2 + 6CO$ *Dodecane breakdown* (8)

These reactions can be used individually or combined into a single fuel breakdown reaction for a gas mixture by applying the respective mole fractions of each component and adding the mole fraction weighted reactions terms together to form a single fuel breakdown reaction for the mixed fuel. For example, combustion of a flare gas mixture of ethylene and propylene could be approximated by combing the individual fuel breakdown reactions for ethylene (Eq.1) and propylene (Eq. 7) using the mole fractions of each specie in the gas mixture.

For even more complex hydrocarbons, the fuel could be approximated by breaking down the complex hydrocarbon into CO, C_2H_2, H_2 and H_2O with stoichiometric coefficients estimated using three rules:

- Heavy sooting hydrocarbons produce more C_2H_2 and possibly a small amount of soot,
- The heat release for primary fuel breakdown should be adjusted by producing more H_2O for higher heat release or more H_2 for less heat release, and
- The oxygen consumption balance, and associated CO production should be determined by an elemental balance.

Testing this approach has shown that the combustion model based on methane combustion has mild sensitivity to the primary breakdown reactions, which allows flexibility in developing advanced combustion models for mixed flare gases. Testing the combustion model in a range of different flame/flare simulations showed that secondary reactions are mostly determined by the flame temperature and soot production.

$H_2 + 0.5O_2 \rightarrow H_2O$ *Hydrogen combustion* (9)

$C_2H_2 + 0.9O_2 \rightarrow 1.8CO + H_2 + 0.01C_{20\ (soot)}$ *Acetylene combustion/ soot nucleation* (10)

$C_2H_2+0.01C_{20\,(soot)} \rightarrow H_2+0.11C_{20\,(soot)}$	*Acetylene/soot combustion/ soot growth*	(11)
$CO + 0.5O_2 \rightarrow CO_2$	*CO combustion*	(12)
$C_{20\,(soot)} + 10O_2 \rightarrow 20CO$	*Soot combustion*	(13)
$CH_4 + 0.5O_2 \rightarrow 2H_2 + CO$	*Methane combustion*	(14)
$C_2H_2 + 3H_2 \rightarrow 2CH_4$	*Forward Acetylene-Hydrogen-Methane Equilibrium*	(15)
$2CH_4 \rightarrow C_2H_2 + 3H2$	*Reverse Acetylene-Hydrogen-Methane Equilibrium*	(16)
$C_2H_4 + H_2O \rightarrow CO + 0.5C_2H_2 + 0.5H_2$	*Ethylene – Water Reforming*	(17)
$C_{20\,(soot)}+20H_2O \rightarrow 20CO+20H_2$	*Soot – Water Reforming*	(18)

One advantage of using this approach is that the initial reaction for burning the flare gas has a low activation energy, which allows partial burning and heat release from flare gas combustion. This maintains stable combustion since the partial heat released supports the subsequent reactions, which produce most of the heat and all the soot in the flame.

Similar to previous combustion models developed and used to analyze MPGF [4] [11], the flare gas Arrhenius combustion time scale is combined with the turbulence eddy breakup time scale to yield an overall time scale for each reaction:

$$t_{total} = t_{arrhenius} + t_{turb} = \frac{1}{C_i} = \frac{1}{A_k T^b exp^{-\left(\frac{T_A}{T}\right)}} + \frac{C_{eb}\Delta x^2}{\varepsilon_{diff}} \tag{19}$$

where $\boldsymbol{A_k}$ is the pre-exponential coefficient, $\boldsymbol{T_A}$ is an activation temperature, $\boldsymbol{T}$ is the local gas temperature, and $\boldsymbol{b}$ is a global exponent, $\boldsymbol{\Delta x}$ is the characteristic cell size, $\boldsymbol{C_{eb}}$ is a user input constant (~0.2E-04) that is cell size dependent, $\boldsymbol{\varepsilon_{diff}}$ is the eddy diffusivity from the turbulence model, and $\boldsymbol{t_{turb}}$ is the turbulence time scale (characteristic time required to mix contents in computational cell). The reaction rates are combined by simple addition of time scales. Depending on the scale of the Arrhenius time scale verses the turbulent time scale, the characteristic time for each reaction may be different. Using this approach, the combustion model approximates turbulent combustion using the Eddy Dissipation Concept (EDC) and local equivalence ratio effects. The Arrhenius kinetics and turbulent mixing approach are like the commonly used Eddy-Breakup (EBU) combustion model.

Based on this approach, a multi-step chemical reaction model is developed using the breakdown reactions (Eqs. 1-8) and the secondary combustion reactions (Eqs. 9-18) for the flare gas to be burned in a MPGF (see Figure 2). All rate equations are solved simultaneously for each reaction and the stoichiometric coefficients are used as constraints that couple the equations and insure conservation of energy and chemical species.

In current MPGF simulations, the global reaction mechanism described by Suo-Anttila, 2019 [3] is used. Suo-Anttila's work relies on previous work by Duterque *et. al.* 1981 [12] and Kim and Maruts, 2006 [13] as starting points. However, since these authors adjusted their global reaction coefficients to match "laminar" flame speed data and since the combustion occurring in a MPGF flame is governed by turbulent mixing, the original coefficients had limited applicability. The coefficients associated with the activation temperature and the exponents for mole fractions were based on the physics of the reaction mechanism thus were not expected to be affected by local grid structure. However, this is not the case for the pre-exponential coefficient. To match reaction rates to measured combustion rates, the pre-exponential coefficients for all the reactions were adjusted to establish a validated combustion model. Also, since the combustion model depends on turbulent mixing of flare gas, combustion is expected to be governed by turbulent mixing of flare gas and ambient air. The *C3d* code uses an LES formulation to approximate turbulent mixing, which depends upon two additional factors, a proportionality coefficient and a cell size. The recommended LES proportionality coefficient of 0.15 was used. To capture the cell size dependency correctly, the same computational mesh characteristic dimensions was used in the full flare mesh as used in the triple ethylene flare radiation validation test (see Figure 9) and the earlier single flare tip test (see Figure 10). Using this information, the required kinetic parameters listed in Table 1 were determined to establish a validated combustion model for the present work.

Figure 9 – Comparison of Predicted and Measured Flame Shape for the 3-Flare Test (sequential predicted images overlaid to test flame)

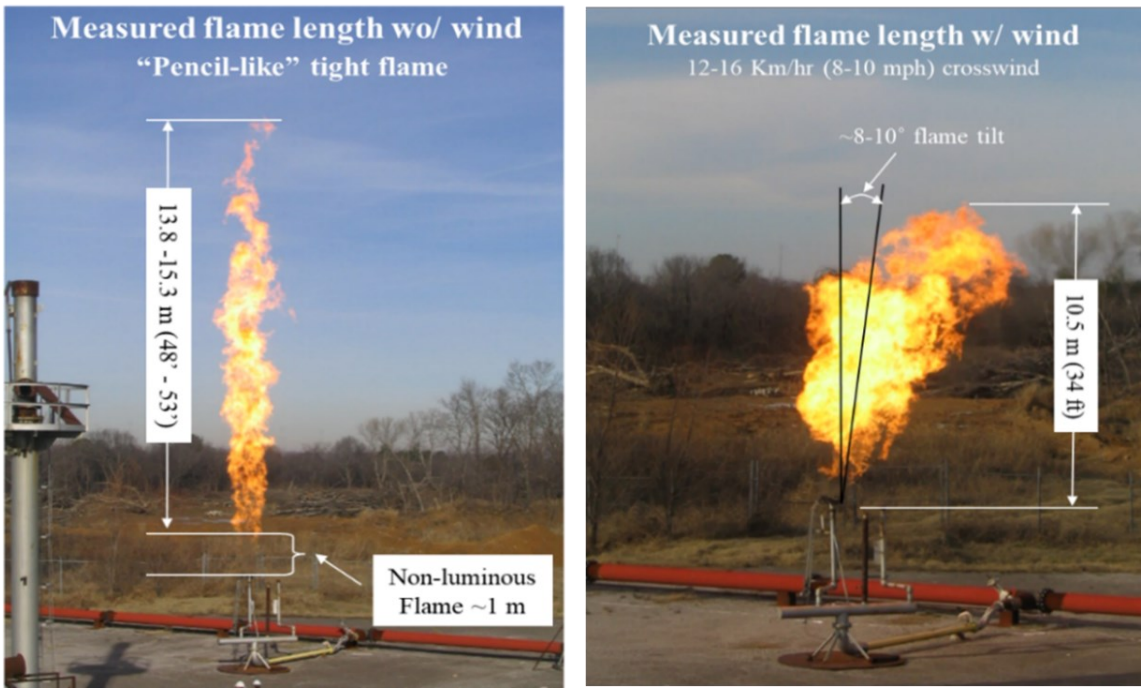

Figure 10- Wind effects on the flame shape of single flare tip with propane flow rate: measured at 1.4 in-wc @ 57 ˚F across orifice plate (7.3 psig tip pressure on 0.457m pipe) [4]

Table 1 - Reaction parameters used in MPGF combustion model

Reaction	f_1	f_2	T_A (K)	C (1/s)	B
Primary Fuel Breakdown (ethylene)	$[C_2H_4]^{0.1}$	$[O_2]^{1.65}$	0 K	1	2
Hydrogen Combustion	$[H_2]^{0.33}$	O_2	10000 K	1e8	0
Acetylene combustion & soot nucleation	$[C_2H_2]^{0.33}$	O_2	15110 K	2e8	2
Acetylene + soot growth	$[C_{20}]^{0.33}$	C_2H_2	15110 K	1e7	0
CO – Oxygen combustion	CO	$[O_2]^{0.25}[H_2O]^{0.5}$	20142 K	1e18	0
Soot combustion	$[C_{20}]^{0.33}$	O_2	0 K	0.5	0.75
Methane combustion	CH_4	O_2	15000 K	1e12	0
Forward Acetylene – Hydrogen – Methane	C_2H_2	H_2	15110 K	5e7	0
Reverse Acetylene – Hydrogen - Methane	CH_4	CH_4	23500 K	4e9	0
Ethylene - Water Reforming	C_2H_4	H_2O	15000 K	5e6	0
Soot – Water Reforming	$[C_{20}]^{0.1}$	$[H_2O]^{1.7}$	0 K	1.0	0.75

Modeling Turbulent Mass Transport and Mixing

C3d is based on a Large Eddy Simulation (LES) formulation to approximate the turbulent reacting flow system. The governing equations for this LES based CFD tool, assuming incompressible fluid flow, are given below [7]:

The steady-state continuity equation is:

$$\partial(\rho u_i)/\partial x_j = 0 \tag{20}$$

where ρ is the density of the gas (mixture) and u is the three-dimensional velocity vector.

The momentum equation is:

$$\partial(\rho u_i u_i)/\partial x_j = \partial P/\partial x_i + \partial \tau_{ij}/\partial x_j + \rho f_i \tag{21}$$

with f_i as the body forces, P as the pressure, and τ_{ij} represented as the stress defined as:

$$\tau_{ij} = \mu\left(\partial u_i/\partial x_j + \partial u_j/\partial x_i\right) + (\mu_B - 2/3\,\mu)\,\partial u_k/\partial x_k \delta_{ij} \tag{22}$$

The other governing equation solved in C3d is the energy equation:

$$\rho\, c_p\ \partial(T)/\partial x_j = -(\nabla . q) - \left(\frac{\partial \ln \rho}{\partial \ln T}\right)\frac{Dp}{Dt} - (\tau : \nabla v) \tag{23}$$

where Cp is the specific heat. The energy equation is used to capture the temperature changes due to combustion and mixing. The energy equation also includes radiation effects.

To resolve sub-filter scales for LES turbulence model, the Gaussian filter is used as shown in equation:

$$G(x - r) = [\![(6/(\pi \Delta \hat{}\, 2\,))]\!]\hat{}\,(1/2)\ \exp\left(-(6(x - r)\hat{}\,2)/\Delta \hat{}\, 2\,\right) \tag{24}$$

The following equations are used to simulate the kinetic energy dissipation on subgrid scales to molecular diffusion:

$$\tau_{ij}^r - 1/3\,\tau_{kk}\delta_{ij} = -2\nu_t \bar{S}_{ij} \tag{25}$$

$$\bar{S}_{ij} = 1/2\,\left(\frac{\partial \bar{u}_i}{\partial x_j} + \frac{\partial \bar{u}_j}{\partial x_i}\right) \tag{26}$$

with τ_{ij}^r as the stress tensor, $\bar{S}_{ij}$ as the rate-of-strain tensor, and ν_t as the turbulent eddy viscosity. The eddy viscosity is approximated as the characteristic length scale times the velocity scale in the subgrid scale model as implemented in the Smagorinsky-Lilly model:

$$\nu_t = (C_s \Delta_g)^2 \sqrt{2\bar{S}_{ij}\bar{S}_{ij}} = ((C_s \Delta_g)^2 |S|, \qquad C_s = \text{Constant}, \qquad \Delta_g = \text{grid size}$$

The equilibrium assumption was applied between energy production and dissipation of small scales in this model.

The multi species conversation equations form is shown in equation (14)

$$\frac{\partial \rho m_i}{\partial t} + \nabla . \rho V m_i = -\nabla . \vec{J}_i + R_i + S_i \quad (27)$$

where, m_i is the mass fraction of species i, $\vec{J}_i$ is the diffusion flux of species i, R_i is the mass creation or depletion by chemical reactions, and S_i mass source. The species equations are solved to keep track of the distribution and concentration of fuel, oxygen, intermediate species, soot, and products of combustion (CO_2 and H_2O). The combustion model was used to provide the species equations source and sink terms as a function of species concentrations, local gas temperature, and turbulent diffusivity.

Modeling Flame Radiation

C3d also includes sub-models to predict flame emissivity as a function of molecular gas composition, soot volume fraction, flame size, shape, and temperature distribution which in turn depend on solutions to the mass, momentum, energy, and species transport equations. The radiation transport model is used not only to predict radiation flux on external (and internal) surfaces, but it also provides source and sink terms to the energy transport equation so that the flame temperature distribution can be accurately predicted.

Thermal radiation effects in *C3d* are calculated in two ways. Within the flame zone, radiation is assumed to be diffusive and outside the flame zone radiative transport is calculated using view-factor methods. The flame surface used in the view-factor calculation is set by finding the dynamic surface wherein a product of hydrocarbon combustion, typically carbon dioxide, has a mass fraction above and below a user specified value, typically 0.04. This dynamic surface, its temperature, and a correction factor (dependent upon flame optical thickness) are all used to calculate view-factor radiation from all flame surfaces to surrounding objects including nearby process instruments, equipment, and structures to identify safe work zones. The view-factor radiation calculation also includes shadowing due to intervening objects. It also includes radiation absorption along the ray path due to participating media including water vapor, carbon dioxide, and soot. Finally, it includes absorption and re-radiation from the ground.

The view-factor radiation calculation has also been implemented in a multi-zone version of C3d to allow multi-Block meshes required for large systems including multiple MPGF systems. The Multi-Block formulation allows the user to split a large problem into separate zones which are coupled together at the boundary conditions. Each zone is solved on a different CPU with time synchronized so large problems requiring 10's to 100's of millions of cells can be solved on multiple CPU's simultaneously to reduce overall computational time. The view-factor thermal radiation from one block (or zone) can be calculated to any geometric position either within or outside that zone. This allows the user to add radiation contributions from adjacent zones to get the total incident radiation value for the entire problem. The only restriction in this zone-to-zone radiation transport method is related to shadowing and media absorption in adjacent zones which is not considered because adjacent zones only know about geometric and compositional details within its own zone boundaries.

Boundary Conditions

Boundary conditions employed in *C3d* include an imposed wind profile on one side of the domain with hydrostatic pressure boundaries on all other sides except the ground where a zero mass-flux boundary was imposed. The thermal and species boundary conditions are set for the specific MPGF firing condition assuming typical air composition with ambient air temperature set to 73˚F (23˚C). Boundary conditions for the flare tips are set using a 1-D grid which connect a point source to the domain. The point source can be set as the individual ports in each tip or can be set as the composite tip. This allows C3d to simulate entire flare fields in an MPGF with hundreds of burners where each burner has many individual ports. This approach captures the flow profile exactly without using greatly refined mesh around the tip which greatly simplifies the calculation and significantly reduces the required CPU time.

Modeling Assumptions

Based on the methodology discussion just given, the following assumptions are used when modeling an MPGF flare:

1. Combustion of the flare gas is approximated by the chemical reaction mechanism described above using specified kinetics (see Table 1).
2. Jet flow from burner tips is approximated using mass sources specified on burner faces.
3. Thermal radiation is calculated using the standard radiation model included in C3d.
4. Ambient wind condition, local flare gas inlet temperature and pressure are matched to local conditions.
5. Mesh refinement is sufficient to provide mesh independent results.
6. Hydrostatic boundary conditions allow flow in and out of the boundaries with wind speed specified according to the prevailing wind data for local conditions.

Code Validation

Predicting heat transfer from the flare flame depends not only on accurate simulation of the combustion chemistry which relates to flame size and shape but also to how heat is transferred from the flame to the surrounding. Most energy from a large MPGF flame leaves with the heated plume but a fraction of it is lost from the flame via radiative heat transfer. Therefore, the radiation model used in C3d, discussed earlier by Smith *et al.* [4], [10], has been re-examined and validated by comparing predicted radiation heat loss from a multi-burner flare flame and predicted values from C3d.

Radiation validation studies have been performed using propylene fuel fired through a similar nozzle tip (see Figure 6) associated with this work. This tip had a 2-in^2 flow area designed for MPGF applications. In this test a single tip was used with 5,465 kg/sec propylene injected at 22.5 PSIG. During the test, the flares were fired into a crosswind with a steady component of 3-7mph gusting to 9-13mph. Radiation was measured at 3 distances (75 ft, 100 ft, and 150 ft) and two elevations (5 ft and 20 ft). The radiometers were placed due east of the flare with the wind blowing from the SSE 169 degrees from true north.

Two simulations were performed considering two wind speeds. As shown earlier [4], flare radiation is very sensitivity to wind speed with a flare flame straight and tall under no wind, but a shorter bushier flame deflected downwind under windy conditions. The wind speeds considered in the validation simulations included a 5mph wind and a 10mph wind to cover the measured wind gusts encountered during the flare test. The simulations also considered atmospheric absorption due to CO_2 and H_2O utilizing the Fuss and Hamins correlation [14].

The C3d simulation considered a 12m square computational domain 20m high (40ft x 40ft x 65ft) with a variable grid composed of 328,000 cells. This simulation required approximately 4 CPU hours from ignition to steady state operation on a standard desktop computer. As shown below (see Table 2) all the measured results fall within the predicted band limited by the two wind speeds. This work reaffirmed how sensitive flare radiation is to wind speed as originally shown by Smith *et al.* 2007 [4].

Table 2 - Comparison of predicted and measured radiation fluxes at 6 locations for 2 wind speeds

Elevation (wind speed) Radiometer distance from flare	5 ft high (3-7mph measured wind) Measured Flux (BTU/hr-ft^2)	5 ft high (5mph predicted wind) Predicted Flux (BTU/hr-ft^2)	5 ft high (10mph predicted wind) Predicted Flux (BTU/hr-ft^2)	20 ft high (3-7mph measured wind) Measured Flux (BTU/hr-ft^2)	20 ft high (5mph predicted wind) Predicted Flux (BTU/hr-ft^2)	20 ft high (10mph predicted wind) Predicted Flux (BTU/hr-ft^2)
75 feet	171	190	168	205	221	183
100 feet	102	117	95	102	120	104
150 feet	34	53	38	34	53	38

CFD Analysis and Results

During an MPGF CFD analysis, individual cases are conducted which examine flare performance nominal (purge) firing rate and maximum (emergency) firing rate with and without wind. Results from these cases are used to evaluate issues related to 1) the effect of tip port area and its consequence on number or tips and tip spacing, 2) the effect or runner to runner spacing, 3) the effect of burner elevation above grade, 4) the effect of wind fence porosity.

To analyze and compare results from CFD cases conducted in the MPGF analysis, a list of flare performance metrics has been identified that related flare performance to design parameters (tip flow area, runner spacing, fence open area) and operating parameters (i.e., flare gas composition, flare gas flow rate). These include:

1. Soot based opacity ISO surface colored by temperature
2. O2 ISO surface colored by velocity magnitude
3. Air supplied to flare burners compared to expected air demand
4. Flare DRE

5. Iso-surface showing unburned flare gas colored temperature
6. 0.05 ppm soot iso-surface colored by temperature
7. CO iso surface of 2000 ppm colored by elevation above grade
8. CO iso-surface of 2000 ppm * carbon count of the fuel colored by elevation
9. Fence surface temperature (K) with x, y, z coordinates of peak temperature
10. Ground surface temperature (K) with x, y, z coordinates of peak temperature
11. Fence radiation flux (W/m2) with x, y, z coordinates of peak flux
12. % Radiation from Flame
13. Wind streamlines showing impact on burners
14. Ground incident radiation (W/m2) with x, y, z coordinates of peak radiation
15. Reverse streamlines from flame surface

A few simulation results from previous work illustrate using *C3d* to analyze various MPGFs. These results show how this tool has been used to explore MPGF design and operation issues. Based on these results, general design and operating guidelines have been identified. Interested readers can find more details of each analysis in previous AFRC papers.

Total Air Demand and Wind Fence Radiation [4]

A MPGF was analyzed for the peak flow condition and a sustained mixed gas condition without crosswind. The computational domain (see Figure 11) for this analysis extended 10m beyond the fence in all directions with an overall height of 25m. Results were used to evaluate the total air demand by the MPGF and radiation flux from the flare to the wind fence.

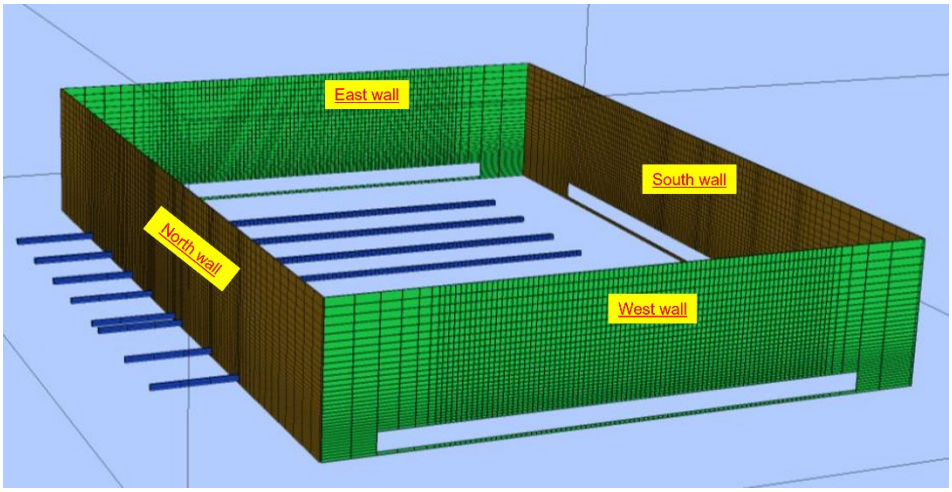

Figure 11 - MPGF geometry from 2007 study

The total air demand was evaluated by summing mass flow crossing a box drawn around the flare burners. The box was located 20 m above grade with vertical planes surrounding the flare burners. Without a crosswind, flow from the top of the box was used to quantify total air demand, since all other faces had inflow. The total air demand for each case is presented in Table 1.

Table 3 - Predicted air demand for MPGF

Case Description	Evaluation Plane Area (m^2)	Total Air Flow (kg/s)	Fuel Flow (kg/s)	Air/Fuel Mass Ratio
Full Field Peak Flow Ethylene	3226	9700	262.3	37
Full Field Sustained Flow Mixed Gas	1843	4800	93.6	51.3

The predicted thermal radiation flux from a MPGF must account for radiation attenuation occurring between the radiating source (flame) and the absorbing media (wind fence, ground, nearby equipment). When radiation passes through adjacent flames some of the radiation is absorbed and re-radiated in other directions. The radiation calculation accounts this using the optical thickness of the intervening flames. The radiation calculation also accounts for absorption and re-emission from absorbing surfaces (i.e., gravel, runner, etc.). Predictions of radiation flux incident on the wind fence ranged between 35,000 W/m^2 to 61,000 W/m^2 for the Peak Flow case and up to 6,600 W/m^2 for the Sustained Flow case.

Table 4 - Radiation flux to wind fence

WALL / CASE	North Wall W/m^2	South Wall W/m^2	Flame Optical Thickness
Peak 944 T/hr Ethylene Flow No Wind	61,000	35,000	0.275
Sustained 337 T/hr Mixed Gas Flow No Wind	6,600	6,600	0.28

Multiple MPGFs Operated Together [15]

A MPGF system firing $6x10^6$ kg/hr of vented gas through 469 flare tips in two adjacent flare fields with air-assisted tips in the center of the flare field operated with an 8m/s cross wind (see

Figure 12). The CFD analysis showed the vortices formed inside the flare due to the wind were relatively weak due to sufficient air influx through the porous fence. MPGF performance was predicted to be good at maximum gas flow, but some regions appeared air-starved with the prevailing wind direction and speed.

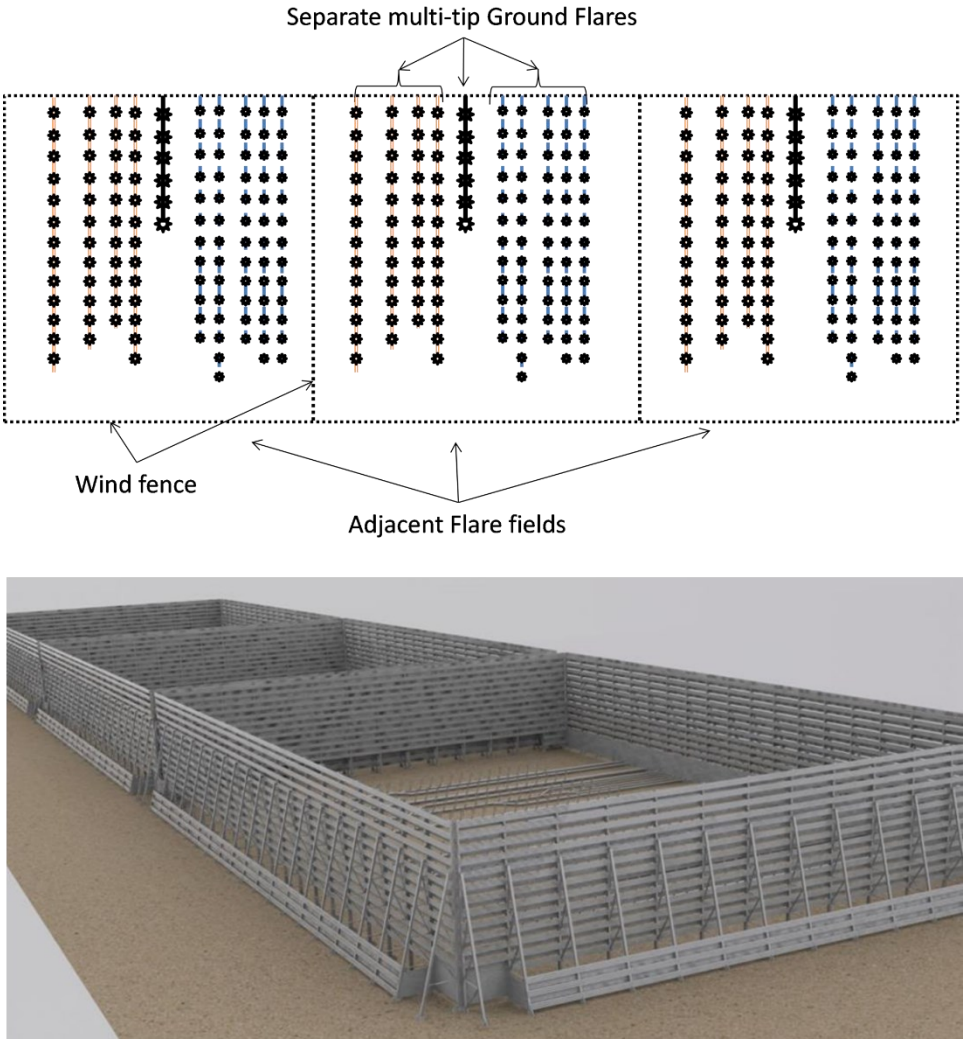

Figure 12 - MPGF design with multiple flare fields and air assisted tips

The "wind-only" portion of this simulation was run for 60 seconds to provide a steady wind profile for the combustion portion of the analysis. Using flow streamlines during the wind-only simulation showed the wind fence allowed sufficient air into the field to prevent strong vortices from forming due to the relative wind direction and flare field orientation (see Figure 13). During the burn time portion of this simulation, results indicated a "quasi-steady" combustion condition was achieved after approximately 5 seconds run time. With combustion, vortices formed by the fence corners did not force flames below the flare burners in the fields.

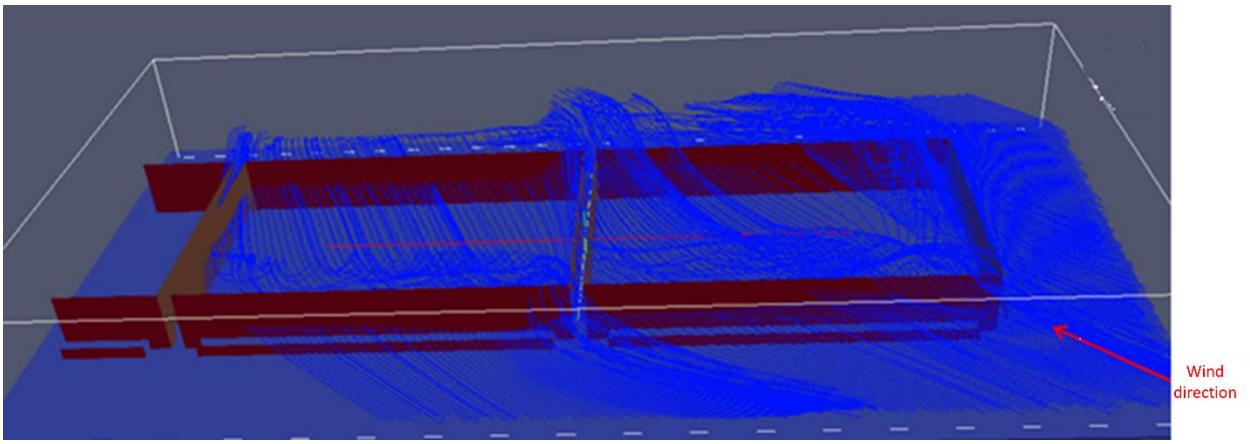

Figure 13 - MPGF wind fence performance

This analysis identified regions in the flare field which appeared to be air-starved that resulted in taller flame heights. It appeared that the air-assisted flare tips did not receive sufficient air from the blower to supply sufficient oxygen to complete flare gas combustion for these tips. These larger flames above the air-assisted tips also impacted the flare burners downwind of the air-assisted tips as well.

Transient Ignition and Flare DRE [5]

MPGF burn flammable hydrocarbon gases from chemical processing and petrochemical refining units. These flares involve hundreds of flare burners arranged along burner runners, operated in a staged fashion to allow safe and efficient processing of large flows of flammable hydrocarbon gases. The wind fences surrounding these flare systems are designed to allow sufficient air into the flare field to reduce smoke formation and reduce radiation flux levels associated with soot radiation. Safe operation is a significant concern due to potentially high radiation flux to the wind fence and surrounding equipment and to nearby work zones. The potential for a high-pressure wave caused by non-standard ignition is also a significant safety concern. The impact of burner-burner spacing on cross lighting when wind is blowing along and perpendicular to the burner runners has been analyzed with results used to assess potential over-pressure conditions.

During MPGF ignition, flare gas exits each burner tip with insufficient momentum to properly mix flammable gas with sufficient oxygen to completely burn. This initial poor mixing results in excessive soot or smoke formation. Practical experience confirms the flare ignition process generally lasts between 10-30 seconds (from flow initiation to steady combustion). Destruction efficiency can be used to quantify flare performance with the MPGF DRE estimated from:

$$DRE(\%) = (1 - \frac{X_{plume}}{X_{in}})x100 \quad (28)$$

where DRE(%) is the destruction and removal efficiency (%), X_{plume} is the species mass flow X found in flare plume after combustion and X_{in} is the species X mass flow in flare gas entering the flare. The importance of this issue can be shown by assuming a conservative estimate of MPGF DRE during ignition as 50%. For a typical MPGF flare that burns 1000 tons/hr of flammable hydrocarbon gas, a 50% DRE during one 30 second ignition event each week results in approximately 866,666 lbs unburnt hydrocarbon per year. Thus, improving MPGF ignition is an important safety and environmental issue.

Analysis of MPGF ignition behavior has been used to estimate safety risks associated with over-pressure conditions. This has also been used to estimate environmental risks based on predicted MPGF DRE. Results from both ignition behavior and estimated DRE can be used to optimize MPGF flare design.

SUMMARY AND CONCLUSIONS

This paper has described *C3d* - the CFD tool used to analyze MPGF performance. Several examples have been given which illustrate how this tool has been used over the years to analyze various MPGF designs operated with and without cross winds blowing on the flare fields. This paper has also shown examples from past studies that highlight various issues related to safe and efficient MPGF design and operation. Future work using this tool will focus on developing a general set of MPGF design guidelines to assist MPGF vendors and end users as well. Specific guidance will focus on

- Tip spacing
- Row spacing
- Firing rate
- Fence design
- Locating surrounding equipment and establishing safe work zones

In summary, CFD analysis of MPGFs conducted over the past fifteen years has shown potential failure modes and safety risks associated with MPGF. These guidelines will be designed to help ensure future MPGF will have less risk and be more capable of processing large amounts of hydrocarbon fuels safely and efficiently.

REFERENCES

[1] J. Smith, Jackson, R.E., Z. Smith, D. Allen and S. Smith, "Transient Ignition of Multi-Tip Ground Flares," in *AFRC Combustion Symposium*, University of Utah, Salt Lake City, Utah, September 17- 19 (2018).

[2] M. Greiner and A. Suo-Anttila, "Validation of the ISIS Computer Code for Simulating Large Pool Fires Under a Varity of Wind Conditions,," *ASME J. Pressure Vessel Technology,* vol. 126, pp. 360-368, 2004.

[3] A. J. Suo-Anttila, "C3d Combustion Model Validation," Albuquerque, January 2019.

[4] J. Smith, A. Suo-Anttila, S. Smith and J. Modi, "Evaluation of the Air-Demand, Flame Height, and Radiation Load on the Wind Fence of a Low-Profile Flare Using ISIS-3D," in *AFRC-JFRC 2007 Joint International Combustion Symposium*, Marriott Waikoloa Beach Resort, Hawaii, October 21-24, 2007.

[5] J. Smith, R. Jackson, V. Sreedharan, A. Suo-Anttila, Z. Smith, D. Allen, D. DeShazer and S. Smith, "Safe Operation of Adjacent Multi-Point Ground Flares: Predicted and Measured Flame Radiation in Cross Flow Wind Conditions," in *AFRC Industrial Combustion Symposium*, Sheraton Kauai Resort, Kauai, Hawaii, September 9 –11, 2016.

[6] J. Smith, Jackson, R.E., Z. Smith, D. Allen and S. Smith, "Transient Ignition of Multi-Tip Ground Flares," in *AFRC Industrial Combustion Symposium*, University of Utah, Salt Lake City, Utah, September 17- 19 (2018).

[7] J. Smith, B. Adams, R. Jackson and A. Suo-Anttila, "Use of RANS and LES Turbulence Models in CFD Predictions for Industrial Gas-fired Combustion Applications," *Journal of the International Flame Research Foundation,* December (2017).

[8] A. Suo-Anttila, K. Wagner and M. Greiner, "Analysis of Enclosure Fires Using the ISIS-3D CFD Engineering Analysis Code," in *12th International Conference on Nuclear Engineering*, Arlington, Virginia, April 25-29, 2004.

[9] J. Smith, A. Suo-Antilla, S. Smith and J. Modi, "Evaluation of the Air-Demand, Flame Height, and Radiation Load on the Wind Fence of a Low-Profile Flare Using ISIS-3D," in *AFRC-JFRC 2007 Joint International Combustion Symposium*, Marriott Waikoloa Beach Resort, Hawaii, 21 - 24 October, 2007.

[10] J. Smith, R. Jackson, A. Suo-Anttila, K. Hefley, Z. Smith, D. Wade, D. Allen and S. Smith, "Radiation Effects on Surrounding Structures from Multi-Point Ground Flares," in *AFRC Industrial Combustion Symposium*, Historic Fort Douglas Officers Club University of Utah, Salt Lake City, Utah, September 9-11, 2015.

[11] J. Smith, A. Suo-Antilla, N. Philpott and S. Smith, "Prediction and Measurement of Multi-Tip Flare Ignition," in *American Flame Research Committees - International Pacific Rim Combustion Symposium, Advances in Combustion Technology: Improving the Environment and Energy Efficiency*, Sheraton Maui, Hawaii, September 26 –29 (2010).

[12] J. Duterque, B. Roland and H. T., "Study of Quasi-Global Schemes for Hydrocarbon Combustion," *Combustion Science and Technology,* vol. 26, no. 1-2, pp. 1-15, 1981.

[13] I. Kim and K. Maruts, "A Numerical Study on Propagation of Premix Flames in Small Tubes," *Combustion and Flame,* vol. 146, pp. 283-301, 2006.

[14] S. Fuss and A. Hamins, "An estimate of the correction applied to radiant flame measurements due to attenuation by atmospheric CO2 and H2O," *Fire Safety Journal,* vol. 37, pp. 181-190, 2002.

[15] J. Smith, R. Jackson, A. Suo-Anttila, K. Hefley, D. Wade, D. Allen and S. Smith, "Prediction and Measurement of Multi-Tip Flare Ignition," in *" American Flame Research Committees 2013 – Industrial Combustion Symposium, Safe and Responsible Development in the 21st Century* , Sheraton Kauai, Hawaii, September 22 –25, 2013.